

Effect of absorbed moisture on the atmospheric plasma etching of polyamide fibers

Lu Zhu^{a,b,c}, Weihua Teng^{a,b,c}, Helan Xu^{a,b,c}, Yan Liu^{a,b,c}, Qiuran Jiang^{a,b,c},
Chunxia Wang^{a,b,c,d}, Yiping Qiu^{a,b,c,*}

^a Key Laboratory of Science & Technology of Eco-Textile, Ministry of Education, China

^b Key Laboratory of Textile Science and Technology, Ministry of Education, China

^c College of Textiles, Donghua University, Shanghai 201620, China

^d College of Textiles and Clothing, Yancheng Institute of Technology, Jiangsu 224003, China

Received 15 May 2007; accepted in revised form 17 August 2007

Available online 1 September 2007

Abstract

A potential problem for the atmospheric pressure plasma treatment is that the moisture absorbed by the substrate may influence plasma surface modification processes. This study evaluated the effect of moisture regain on the surface morphology change of polyamide fibers by plasma etching. Polyamide 6, poly(*p*-phenylene terephthalamide) (PPTA, aromatic polyamide), wool (polyamide 2), and ultrahigh modulus polyethylene (UHMPE, polyamide infinity) fibers, were selected to represent various polyamide molecular structures. The fibers were plasma treated at three moisture regains corresponding to three different relative humidity levels (10, 65, and 100%). Scanning electron microscope (SEM) showed that no apparent morphology change was observed on the surface of UHMPE and PPTA fibers. Under the nano-scale surface analysis of atomic force microscopy (AFM), however, rougher surface of UHMPE and PPTA fibers appeared with elevated relative humidity or higher moisture regain. In terms of polyamide 6 and wool, SEM images revealed that compared to the slight plasma etching effect of fibers with the lowest moisture regain, a thin surface layer of the treated fibers with higher moisture regain was partially or completely peeled off. It may be concluded that fiber moisture regain plays an important role in atmospheric pressure plasma etching of polyamide fibers, which may be mainly due to the interaction between the absorbed water and the polymer molecules. It can be concluded that the etching rate of atmospheric pressure plasma for a polymer depends on its moisture regain, intermolecular forces, crystallinity, and molecular structure.

© 2007 Elsevier B.V. All rights reserved.

Keywords: Atmospheric pressure plasma; Plasma etching; Moisture regain; Polyamide; SEM

1. Introduction

As an environmentally favorable alternative, plasma technology has been applied effectively in modifying surface properties of polymers [1–3]. However, most plasma treatments have been carried out at very low pressure, or in vacuum system, which need expensive and complicated vacuum equipment [3]. In addition, for hygroscopic materials, the substrates have to be dried before the plasma treatment so as to quickly reach required degree of vacuum, which could be time and energy consuming [4].

In recent years atmospheric pressure plasma treatments have been introduced to overcome this problem [5,6]. It works under open environment and the treated materials are relatively less restricted [7]. With the high energy particles excited at the

Table 1
Chemical structures of the four fibers

Sample	Chemical structure
UHMPE	$\text{-(CH}_2\text{-CH}_2\text{)}_n\text{-}$
PPTA	$\text{-(NH-}\langle\text{benzene ring}\rangle\text{-NHCO-}\langle\text{benzene ring}\rangle\text{-CO)}_n\text{-}$
PA 6	$\text{-(NH-(CH}_2\text{)}_5\text{-CO)}_n\text{-}$
Wool	$\text{-(NH-CHR}_1\text{-CONH-CHR}_2\text{-CO)}_n\text{-}$ (R ₁ and R ₂ are α side chain of aminophenol)

* Corresponding author. Key Laboratory of Textile Science and Technology, Ministry of Education, China. Tel.: +86 21 67792744; fax: +86 21 67792627.

E-mail address: ypqiu@dhu.edu.cn (Y. Qiu).

Table 2
Moisture regains of the four fibers corresponding to 10, 65, 100% RH, respectively

Sample	Moisture regain (%)		
	Corresponding to 10% RH	Corresponding to 65% RH	Corresponding to 100% RH
UHMPE	0	0	0
PPTA	0.50	4.50	5.50
PA 6	1.23	5.19	9.70
Wool	4.51	12.1	26.6

ambient temperature, the atmospheric pressure plasma can be used to treat the surface of materials with different structures and chemical reactivity while bulk of materials maintain unchanged [8]. There is a potential problem for atmospheric pressure plasma treatment on hygroscopic materials especially those used in textiles. Because the moisture regain (MR) of these materials will change with the relative humidity (RH) of the environment, it may influence the effects of the atmospheric pressure plasma treatments as reported in our previous studies [9–11].

Under the bombardment of active species generated by a homogeneous plasma, a polymer surface can be changed by removal of surface contaminations [12,13], introduction of new chemical functional groups [14–17] or deposition of a thin

coating [18–21]. Plasma etching is to remove a weak boundary layer near the surface of the polymers or the low-molecular-weight fragments formed as a result of chain scission [3,22–25]. The predominant active species in radio frequency plasma are positive ions and photons, with ability of breaking primary chemical bonds and inducing cross-linking [26,27]. The extent of degradation in plasma etching is closely correlated to the chemical structure of the polymer at a given plasma working condition [5,28–32]. It was reported that polymeric structures containing oxygen were more susceptible to plasma while polymers with high crystal and stable structures were more resistant to oxidation and etching [30,32]. However, little has been reported in literature on the influence of absorbed moisture in polymeric materials on the etching of atmospheric pressure plasma treatment, partially because this has not been a problem in the traditional plasma surface modification in vacuum.

This study was aimed to investigate how the moisture regain of typical hygroscopic fibers affects the plasma etching behavior induced by atmospheric pressure plasmas. Four representative fibers, wool fibers, PA 6 and poly(*p*-phenylene terephthalamide) (PPTA) fibers, ultrahigh modulus polyethylene (UHMPE) fibers were selected as model materials. The repeating units of these polymers are shown in Table 1. The first three are typical polyamide (PA) fibers widely used in industry and UHMPE could be considered as a special case of PA.

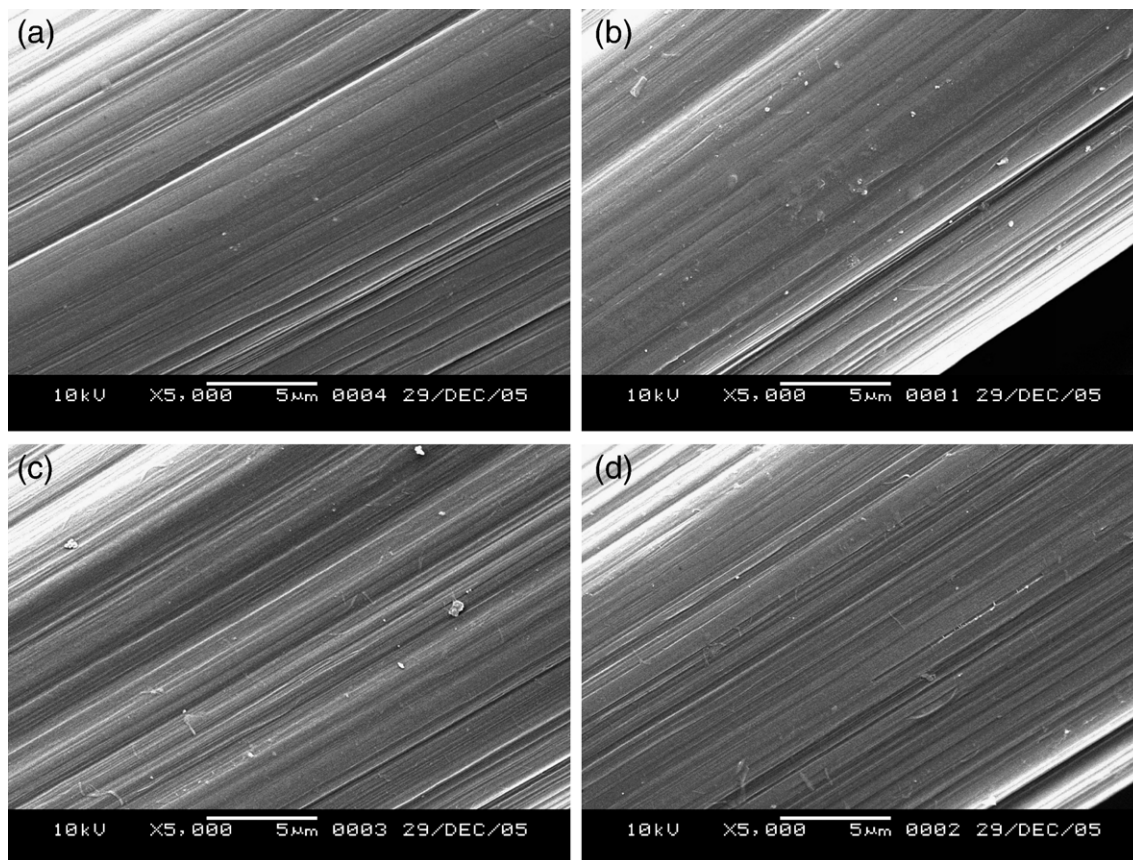


Fig. 1. SEM photos of control and treated UHMPE fibers under 5000 \times magnification: (a) control; (b) treated in 10% RH; (c) treated in 65% RH; (d) treated in 100% RH.

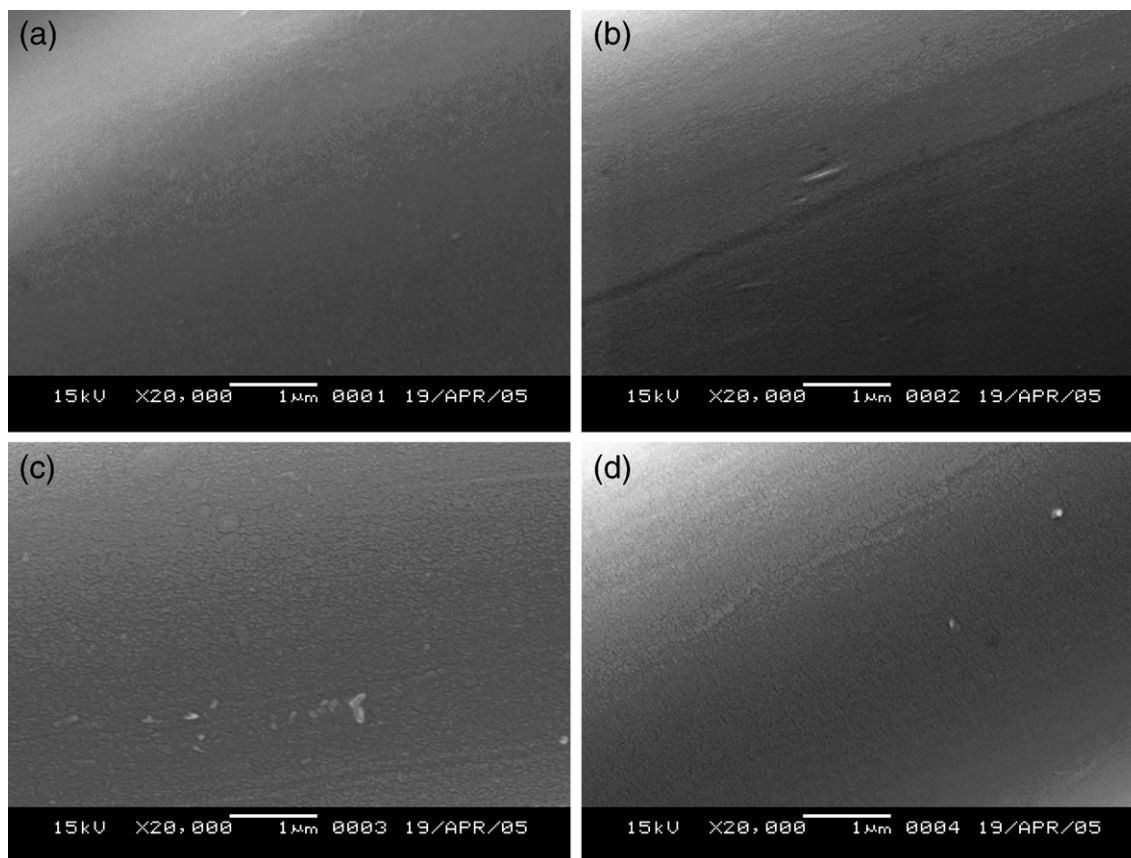


Fig. 2. SEM photos of control and treated PPTA fibers under 20,000 \times magnification: (a) control; (b) 0.50% MR, treated; (c) 4.50% MR, treated; (d) 5.50% MR, treated.

Chemical structure of PA fibers can be described by the common formula:



or



where the former is named as PA ($i+1$) and the latter as PA i , ($j+2$), i , j are integers. PA 6 fiber is one of the most widely used PAs. As another form of PA, *i.e.* a rigid-chain aromatic polyamide, PPTA fiber is increasingly used in the fields of structural composites for aerospace and other reinforcement applications. According to the common formula, wool fiber, can be regarded as PA 2. UHMPE fiber does not contain amide groups in its backbone and therefore cannot be considered PA. However, if one consider the structure of regular PA, it is not too hard to realize that linear PAs, such as PA r or PA 6,6, are nothing but a polymer constructed by inserting amide groups periodically into a polyethylene backbone. In other words, as the distance along the molecular chain between two neighboring amide groups increases, the performance of the PA will be more and more like polyethylene. This is why polyethylene is also selected as a special case of PAs. Results from polyethylene could provide valuable information about how the molecular segments between the two neighboring amide groups corresponding to the plasma treatment. In addition, UHMPE

fiber can be used to test if the moisture in air could significantly affect the plasma etching process since the fiber absorbs very little water, while this effect cannot be evaluated because moisture in the fiber as well as in air could jointly interact with the etching process. Therefore, the four fibers selected in this study represent various polyamide and related molecular structures.

Owing to the variation in molecular structures, the moisture regains of the four fibers are different in a certain RH. The fibers were plasma treated after being conditioned for enough time at pre-designated RH levels. Surface morphology changes of these four fibers treated at different RH with atmospheric pressure plasma jet (APPJ) were observed using scanning electron microscope (SEM) and atomic force microscopy (AFM) methods.

2. Experimental

2.1. Materials

The fibers used in this experiment were PA 6 fibers (provided by Jiangsu Yizheng Chemical Fiber Textile Limited Company, China), wool (Merino, provided Shanghai Third Wool Factory, China), UHMPE fiber supplied by Ningbo Dacheng Company (Zhejiang, China), and PPTA fiber (Twaron[®] 100, provided by Teijin Limited Company, Japan).

Before the plasma treatment, all fibers were washed with acetone for 10 min and dried in a vacuum oven at room

temperature for 24 h to remove the surface finishes and contamination. In order to prepare for samples with different moisture regain, each type of the cleaned samples except UHMPE fibers were divided into four groups respectively. One group was heated in the oven for 1.5 h at 100 °C to evaporate the remaining moisture and then stored in a 10% RH container until the plasma treatment. Another group was suspended above water in a desiccator, which had close to 100% RH. The last two groups were balanced in the standard textile test conditions of 20 °C and 65% RH for 24 h, of which one was used as the control sample and the other was prepared for the plasma treatment.

Table 2 shows the measured moisture regains of the four fibers in the three typical RH levels (10, 65 and 100%) which were chosen in accordance with the three regimes of water absorption described by Nissan [33]. Due to the hydrophobic nature of UHMPE fibers, it was not necessary to precondition the UHMPE fibers in the four different RH levels.

2.2. Plasma treatment

An atmospheric pressure plasma jet (Atomflo™-R, Surfex Company of USA) was employed for the plasma treatment of samples. To initiate plasma, pure helium was chosen as a working gas at a flow rate of 10 L/min and treatment nozzle temperature of

100 °C although the exact composition of the gas mixture in the plasma jet was unknown since it was carried out in atmosphere. The discharge power was 10 W and the radio frequency was 13.56 MHz. In the plasma treatment, the distance between the jet and sample was 2 mm and the samples were moved on a conveying belt perpendicular to the jet at a velocity of 3 mm/s. The movement was repeated twice to obtain homogenous treatment effect. In order to control the relative humidity for the three samples with different moisture regains, the plasma jet and the conveying belt system were kept in a sealed plastic bag as an environment chamber. The environment of the 10% RH was conditioned by putting desiccants into the plastic environment chamber for 12 h. After the plasma treatment under 10% RH condition, the desiccants were removed and water was sprayed into the small environment to raise the RH. Then the RH reached 65% and 100% within half an hour. Of course, regardless how careful we could prepare the experiment, the RH kept changing during the plasma treatments due to certain amount of helium was added into the plastic bag. However, due to relatively short treatment duration and the fact the moisture in the fibers required sometime to defuse out in order to reach new equilibrium with the environment, it was assumed that the moisture in the fiber did not change significantly and was at least proportional to the initial moisture regains of the fibers.

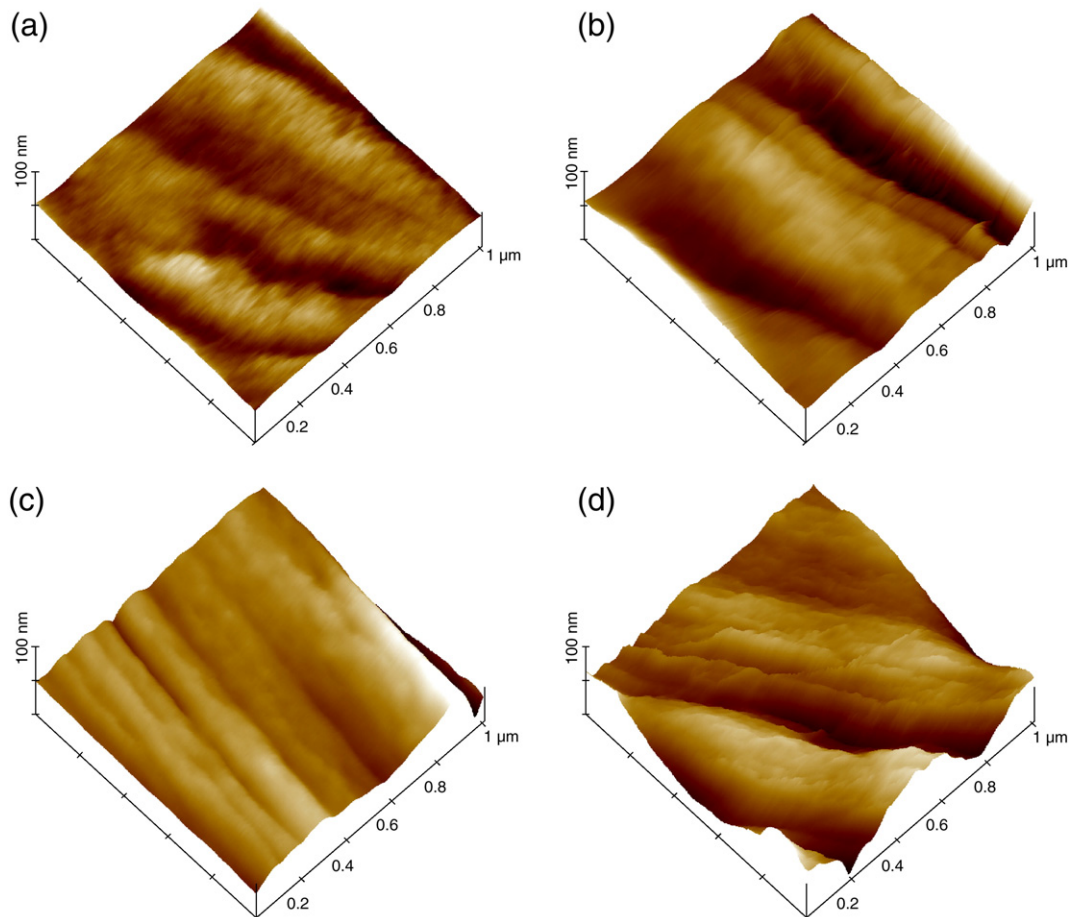


Fig. 3. AFM images of control and treated UHMPE fibers: (a) control; (b) treated in 10% RH; (c) treated in 65% RH; (d) treated in 100% RH.

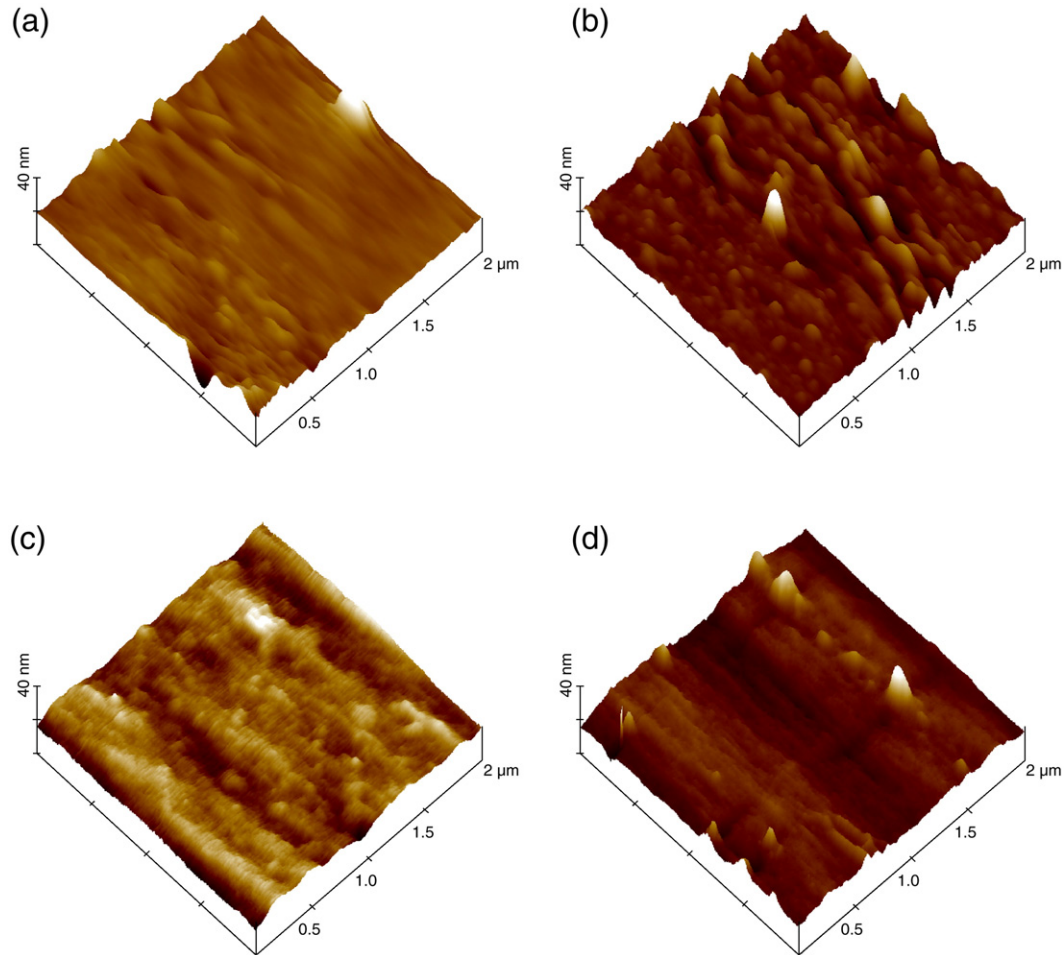


Fig. 4. AFM images of control and treated PPTA fibers: (a) control; (b) 0.50% MR, treated; (c) 4.50% MR, treated; (d) 5.50% MR, treated.

2.3. Surface morphology analysis

The micro-scale and nano-scale surface morphology of the control and the treated fibers were investigated using SEM and AFM respectively. SEM studies were performed in a JSM-5600LV Model at a maximum magnification of 3×10^5 and a voltage of 15 kV. The samples were gold coated before the measurement. AFM experiments were carried out on a MultiMode Digital Instrument Nanoscope III set-up in the contact mode under ambient conditions. The force modulation SPM tip was mounted on the commercial standard silicon-nitride cantilever. It was certified that the surface morphology did not change after consecutive scans at the same region in the repeated AFM measurements.

2.4. Measurement of crystallinity

X-ray diffraction (XRD) patterns of finely powdered samples were recorded using a diffractometer (D/max-2250PC from Rigaku Company, Japan). The diffractometer provided Ni-filtered Cu K α radiation with an accelerating voltage of 40 kV and an anode current intensity of 300 mA. The deflection angle had a range from 4° to 40°, with a 0.1° step and 20-s impulse counting.

3. Results and discussion

3.1. UHMPE fiber and PPTA fiber

The surfaces of UHMPE fibers from the four groups are shown in Fig. 1. There were micro-depth parallel grooves on the surface of all groups. The existence of the grooves was generated by the gel spinning process in fiber production [34]. On the plasma-treated fiber surface, minor etching effect may be seen but the difference among the three treated groups was not obvious. Fig. 2 shows that no apparent etching can be observed in the plasma-treated PPTA fibers.

Table 3

Root mean square (RMS) roughness of untreated and plasma-treated UHMPE and PPTA fiber surfaces

UHMPE	RMS (nm)		PPTA	RMS (nm)	
	Average	SD		Average	SD
Control	1.53	0.34	Control	0.74	0.18
In 10% RH, treated	6.55	0.63	0.5% MR, treated	1.79	0.39
In 65% RH, treated	6.14	1.86	4.5% MR, treated	1.43	0.11
In 100% RH, treated	10.03	3.86	5.5% MR, treated	2.34	0.37

SD = Standard deviation.

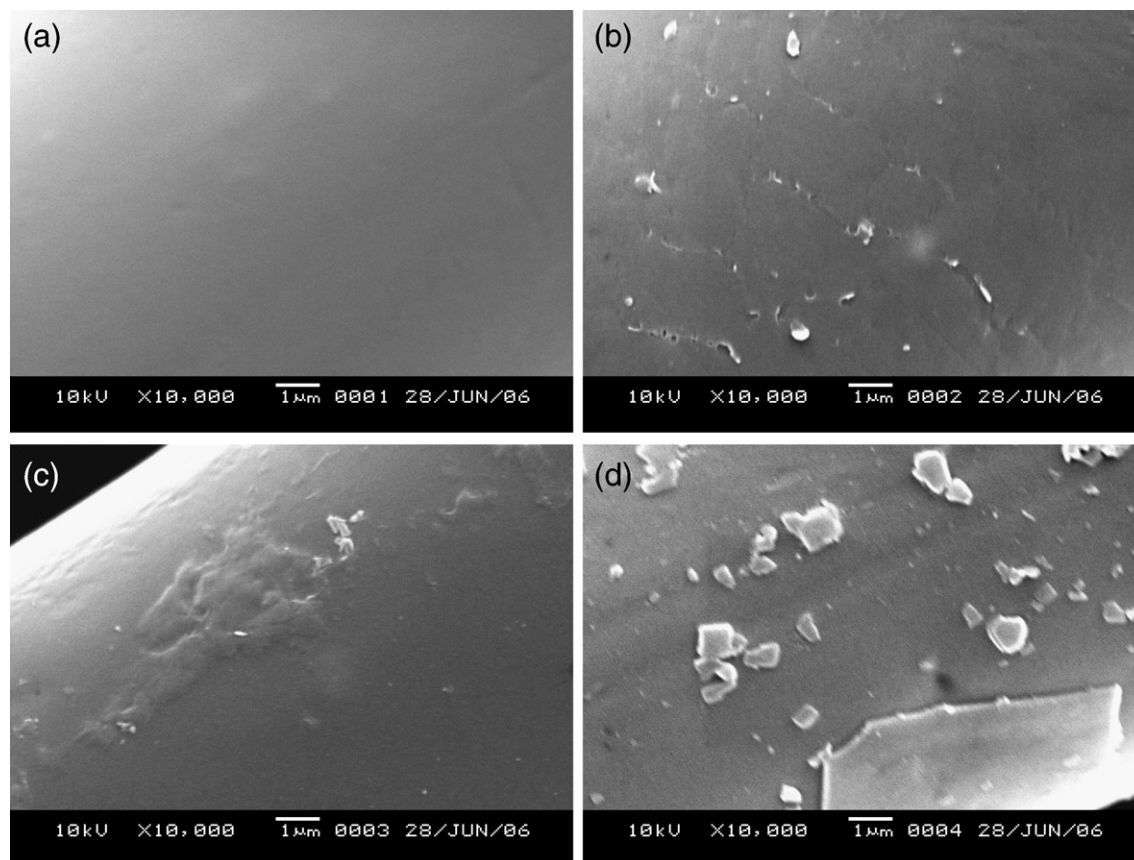


Fig. 5. SEM photos of control and treated PA 6 fibers under 5000 \times magnification: (a) control; (b) 1.23% MR, treated; (c) 5.19% MR, treated; (d) 9.70% MR, treated.

Due to the slight etching effect on the treated UHMPE fibers and PPTA fibers indicated by SEM photos, AFM examination of the same samples was performed. The AFM three-dimensional image profiles illustrated in Fig. 3 (UHMPE fibers) and Fig. 4 (PPTA fibers) are the original scans without any filtering or contrast enhancement. The surface of all fibers was characterized by grooves oriented in the fiber axis direction similar to those shown in the SEM photos.

The control UHMPE fibers presented a relatively smooth topography on the hills of the fiber surface. By contrast, plasma-treated samples displayed somewhat rougher surfaces. It was clear in the images that the surface of the fibers treated in 100% RH was most roughed as the hills were visibly rougher than the rest of the fibers, although the statistical analysis on the root mean square (RMS) roughness (Table 3) could not be carried out due to lack of information on the raw data received by the build-in computer program used to sample and to calculate the means and standard deviations. These results implied that the moisture in air in the high RH environment could possibly enhance the plasma surface etching to the UHMPE fiber. However, the increased roughness is rather minor compared with those observed in the PA fibers.

The AFM images of the control and the treated PPTA fibers also show that new surface topography was induced by the plasma treatment. Increased surface roughness can be observed from the plasma-treated fibers as indicated by RMS roughness (Table 3). This may be due to the fact that raising the

relative humidity or increasing the moisture absorption could make the amorphous region of the fibers looser, and accordingly enhance the susceptibility of the fiber surface to plasma etching. Thus, we may conclude that the moisture in air may not significantly enhance the etching ability of plasmas while the moisture absorbed into the fiber does.

3.2. Polyamide 6 and wool fibers

The SEM results for the control and the treated PA 6 fibers are shown in Fig. 5. It can be seen that atmospheric pressure plasma treatment did etch the fiber surface to different extent for the three treated groups. It was evident that the plasma treatment had a subtle etching effect on the PA 6 fibers with 1.23 and 5.19% moisture regains, although the latter appeared rougher than the former. The most pronounced change was observed in the treated fibers with the highest moisture regain. The plasma treatment peeled off significant amount of materials on the outmost surface layer, leaving only small fragments on the surface.

The surface morphology of wool with different moisture regains exposed to plasma discharge also underwent a significant change, which is illustrated by SEM images in Fig. 6. After the plasma treatment, small quantity of micro-cracks emerged on the surface scales of the 4.51% MR wool fiber, consistent with what was observed in vacuum plasma treatment of wool fibers [35,36]. In comparison, the surface of the 12.1% MR treated fiber suffered a more aggressive ablation,

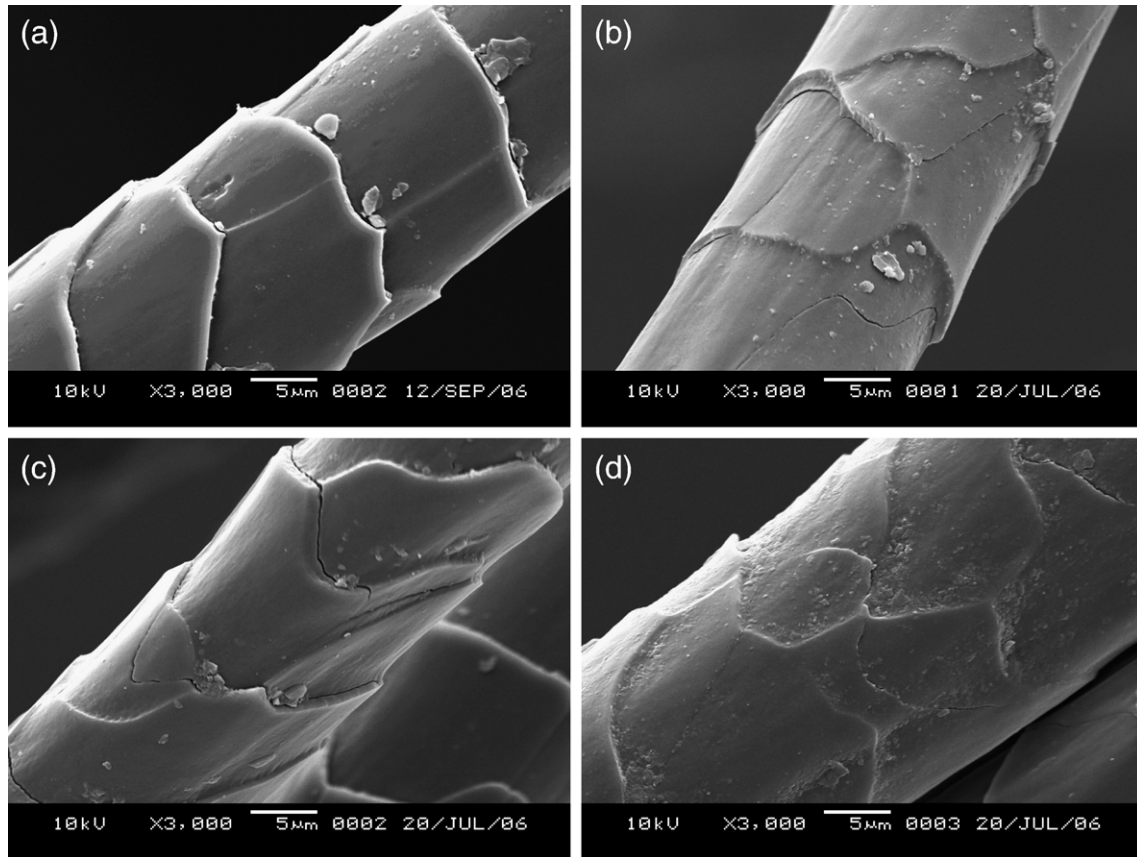


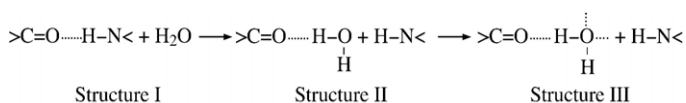
Fig. 6. SEM photos of control and treated wool under 3000 \times magnifications: (a) control; (b) 4.51% MR, treated; (c) 12.1% MR, treated; (d) 26.6% MR, treated.

in which the edge of scales was split (Fig. 6c). For the fibers with 26.6% moisture regain, on the other hand, all scales on the original wool surface were etched away by plasma treatment and a new smooth surface appeared.

3.3. Discussion

In this study, PPTA fibers, PA 6 fibers and wool, all containing amide groups, had displayed diverse etching characteristics in atmosphere pressure plasma treatment when they absorbed different amount of moisture. UHMPE fibers were also used as a basic model without amide groups to evaluate the influence of moisture in air on the plasma etching effect. Increasing moisture regain greatly facilitates the plasma etching for all three hygroscopic PA fibers. This indicates that both the moisture regain and the polymer structure determine the outcome of the interaction between the plasma active species and the polymer surface.

In PA fibers, the linkages between C=O and H-N groups are hydrogen bonds, where the positive H atoms can be attracted to a negatively polarized O atoms in the vicinity, as shown in Structure I.



The hydrogen bonds contribute to the intermolecular force in polyamides, normally with energy of 14.6–21.7 kJ/mol [37]. Upon exposure to a humid environment, water diffuses into the amorphous regions, and the hydrogen bonds between PA chains are disrupted in favor of forming hydrogen bonds between the amide groups and the water molecules, as illustrated in Structure II. It was proposed by Nissan [33] that there was a co-operative phenomenon in the breakage of hydrogen bonds, i.e., one H-bond breakage might trigger a few neighboring bonds to break simultaneously. The amount of absorbed moisture plays an important role in determining the dissociation modes of hydrogen bonds. At low moisture regain, due to a paucity of water molecules, those hydrogen bonds in Structure I that are triggered to dissociate have little chance to keep on breaking, and thus the breakage of H-bonds takes place individually [33]. However, when the moisture regain exceeds the critical moisture regain, more water molecules are available and three further sites for hydrogen bonds are provided (Structure III). This triggers breaking down of hydrogen bonds cooperatively in a cluster. The original regular orderly structure is destroyed, and the weak van der Waal forces, a value of 2–8 kJ/mol, become the new intermolecular forces to maintain the fiber structure. Therefore, a relaxed network structure and a concomitant swelling resulted from the invasion of water molecules could allow molecular chains of the polymer surface easier to be struck off under the bombardment of the activated species in the plasma. This may be one of the major

reasons that higher plasma etching effect was observed when increasing the amount of moisture in hygroscopic fibers.

In semi-crystallized fibers, moisture is not easy to access the densely packed crystalline regions while it is absorbed into the amorphous regions composed of tie-molecules, loose chain loops and ends of macromolecules [38]. Using XRD method, the crystallinities of the four polymers after conditioned in the standard textile testing condition (20 °C and 65% relative humidity) for 24 h were measured, and the calculated results are given in Table 4. According to the etching susceptibility suggested by SEM, it can be seen that higher crystallinity has a negative effect on fastening the plasma etching rate. In order to further explore the influence of moisture regain on crystallinity, the crystalline structure of PA 6 and wool were analyzed by XRD examinations after both fibers were conditioned in 10% and 100% RH for 24 h. The exemplary runs were recorded (Fig. 7) and the calculated crystallinities were obtained (Table 4). The results of examining the crystallinity level indicate that as the moisture regain of hygroscopic fibers increases, the crystallinity of the fiber decreased while the amorphous region is enlarged. Combining this result with the microscopy observation, it may be concluded that decreased crystallinity promotes the plasma etching due to the fact that amorphous region could be etched by plasmas much faster than the crystalline region.

The amide groups are responsible for the amount of water absorption in PAs. The density of amide groups, defined as the number of amide groups (–CONH–) per carbon atom on the backbone chain, can be used to characterize the nature of the PA. For UHMPE, PPTA, PA 6 and wool, the densities of amide group, can be calculated as 0, 0.142, 0.167 and 0.5 respectively. As expected, a positive relationship was found between the amide group density and the plasma etching effect, which is reasonable because more amide groups yield higher moisture regain and severer co-operative dissociation of original hydrogen bonds, and consequently contributes to a more aggressive plasma etching effect.

In comparison with the obvious peeling off of the outmost layer on the surface of the plasma-treated PA 6 and wool fibers as shown in a micro-scale, the surface morphology change on PPTA fibers was mild and only can be seen only on a nano-scale. The greater molecular stiffness and structural stability of PPTA fibers due to the existence of aromatic rings in the backbone may hinder the molecular chain scissions, leading to a greater difficulty for plasma etching. In addition, as a fiber spun from liquid crystalline state, the fiber has high molecular orientation and high crystallinity and thus has small fraction of

Table 4
Crystallinities of the four fibers after conditioned in 10, 65, 100% RH for 24 h, respectively

Sample	Crystallinity (%)		
	10% RH	65% RH	100% RH
UHMPE	–	79.94	–
PPTA	–	58.68	–
PA 6	28.58	27.47	26.92
Wool	21.50	19.52	17.97

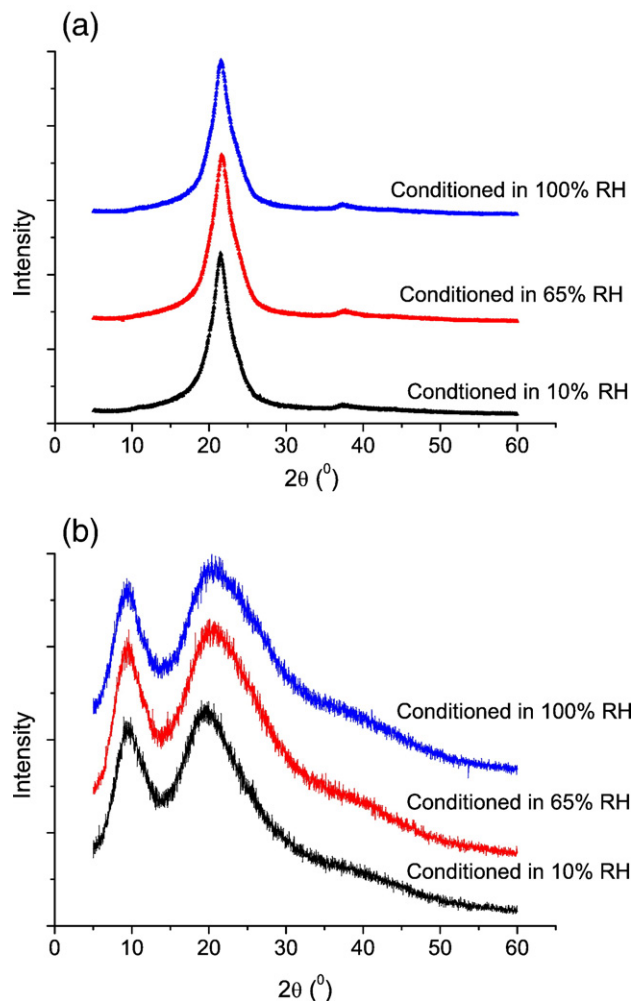


Fig. 7. Diffraction spectra of untreated fibers with different moisture regains: (a) PA 6 fiber; (b) wool.

surface covered by amorphous regions. Therefore it was much harder to be plasma etched.

UHMPE fibers have linear and flexible molecular chains. Manufactured with gel spinning process, the fiber also has high molecular orientation and high crystallinity. Furthermore, UHMPE fibers have no polar functional groups and thus do not absorb significant amount of water. Thus the plasma etching effect was also really minor.

Therefore, besides moisture regain, several other factors, such as intermolecular forces, crystallinity, amide-group density, and molecular structural stability, also play important roles in determining plasma etching effectiveness on PA fibers. By taking into account all these factors influencing the plasma etching effect in this study, a relationship could be obtained as follows:

Plasma etching extent \propto

$$\frac{\text{Moisture regain} \times \text{Amide-group density}}{\text{Intermolecular force} \times \text{Crystallinity} \times \text{Molecular stiffness}}$$

This expression describes that in PAs, enhancing the moisture regain or the amide-group density could promote the

plasma etching while increasing intermolecular forces, crystallinity, and molecular stiffness, would result in a negative effect on the plasma etching rate.

4. Conclusions

The effect of moisture regain or RH on plasma etching of UHMPE fibers, PPTA fibers, PA 6 fibers and wool was investigated. The surfaces of all fibers conditioned in 10% RH were slightly roughed after the plasma treatment. When the PA 6 and wool fibers absorbed enough moisture, the surface layer of the fibers was etched to different extent under the bombardment of active species in the plasma. The plasma etching extent was increased as moisture regain increased and for the PA fibers. Moisture absorbed into the fiber acted as a plasticizer to loosen the molecular structure or to break the hydrogen bonds between two amide groups, facilitating the plasma etching reactions on the polymer surfaces. Meanwhile, other factors including intermolecular forces, crystallinity, amide-group density and molecular stiffness, also took a part in determining plasma etching extent.

Acknowledgements

This project was jointly sponsored by the National High Technology Research and Development Program of China (No. 2007AA03Z101), Shanghai Pujiang Program (No. 06PJ14011), Program for Changjiang Scholars and Innovative Research Team in University (No. IRT0526), and Donghua University Undergraduate Education Reform Program.

References

- [1] H. Höcker, *Pure Appl. Chem.* 74 (2002) 423.
- [2] R. Li, L. Ye, Y.W. Mai, *Compos. Part A* 28 (1997) 73.
- [3] E.M. Liston, L. Martinu, M.R. Wertheimer, *J. Adhes. Sci. Technol.* 7 (1993) 1091.
- [4] C.M. Chan, T.M. Ko, *Surf. Sci. Rep.* 24 (1996) 1.
- [5] Y. Qiu, Y.J. Hwang, C. Zhang, B.L. Bures, M. Mccord, *J. Adhes. Sci. Technol.* 16 (2002) 449.
- [6] T.C. Montie, K. Kelly-Wintenberg, J.R. Roth, *IEEE Trans. Plasma Sci.* 28 (2000) 41.
- [7] C. Tendero, C. Tixier, P. Tristant, J. Desmaison, P. Leprince, *Spectrochim. Acta, Part B: Atom. Spectrosc.* 61 (2006) 2.
- [8] A. Schutze, J.Y. Jeong, S.E. Babayan, J. Park, G.S. Selwyn, R.F. Hicks, *IEEE Trans. Plasma Sci.* 26 (1998) 1685.
- [9] L. Liu, Q. Jiang, T. Zhu, X. Guo, Y. Sun, Y. Guan, Y. Qiu, *J. Appl. Polym. Sci.* 102 (2006) 242.
- [10] Y. Liu, H. Xu, L. Ge, L. Han, H. Yu, Y. Qiu, *J. Adhes. Sci. Technol.* 21 (2007) 663.
- [11] L. Zhu, C. Wang, Y. Qiu, *Surf. Coat. Technol.* 16-17 (2007) 7453.
- [12] S.A. Szekeres, *Vacuum* 51 (1998) 469.
- [13] P. Krüger, R. Knes, J. Friedrich, *Surf. Coat. Technol.* 12 (1999) 240.
- [14] M.G. McCord, Y.J. Hwang, Y. Qiu, L.K. Hughes, M.A. Bourham, *J. Appl. Polym. Sci.* 88 (2003) 2038.
- [15] R.M.A. Malek, I. Holme, *Iran. Polym. J.* 12 (2003) 271.
- [16] J.P. Badey, E. Espuche, Y. Jugnet, T.M. Duc, B. Chabert, *Vide-Science Technique Et Applications.* 272 (1994) 386.
- [17] D.N. Hild, P. Schwartz, *J. Adhes. Sci. Technol.* 6 (1992) 879.
- [18] M. Shaker, I. Kamel, F. Ko, J.W. Song, *J. Compos. Technol. Res.* 18 (1996) 249.
- [19] N. Dilsiz, E. Ebert, W. Weisweiler, G. Akovali, *J. Colloid Interface Sci.* 170 (1995) 241.
- [20] W.J.V. Ooij, S. Luo, S. Datta, *Plasmas Polym.* 4 (1999) 33.
- [21] R. Prikryl, O. Salyk, J. Vanek, V. Cech, *J. Studynka, Czech. J. Phys.* 52 (2002) 816.
- [22] W. Brandl, G. Marginean, *Thin Solid Films* 447 (2004) 181.
- [23] K.K. Wong, X.M. Tao, C.W.M. Yuen, K.W. Yeung, *Text. Res. J.* 70 (2000) 886.
- [24] S.L. Gao, *J. Appl. Polym. Sci.* 47 (1993) 2065.
- [25] S.I. Moon, J. Jang, *Compos. Sci. Technol.* 57 (1997) 197.
- [26] D. Rapp, P. Englander-Golden, *J. Chem. Phys.* 43 (1965) 1464.
- [27] G. Hancock, *Surf. Coat. Technol.* 74-75 (1995) 10.
- [28] Y.J. Hwang, Y. Qiu, C. Zhang, B. Jarrard, R. Stedeford, J. Tsai, Y.C. Park, M. Mccord, *J. Adhes. Sci. Technol.* 17 (2003) 847.
- [29] M. Riekerink, J. Terlingen, H. Engbers, J. Feijen, *Langmuir* 15 (1999) 4847.
- [30] C.M. Weikart, H.K. Yasuda, *J. Polym. Sci., A, Polym. Chem.* 38 (2000) 3028.
- [31] H.M. Powell, J.J. Lannutti, *Langmuir* 19 (2003) 9071.
- [32] V. Sovorcik, K. Kolarova, P. Slepicka, A. Mackova, M. Novotna, V. Hnatowicz, *Polym. Degrad. Stab.* 91 (2006) 1219.
- [33] A.H. Nissan, *Macromolecules* 9 (1976) 840.
- [34] M.S. Silverstein, *J. Appl. Polym. Sci.* 72 (1999) 405.
- [35] I.M. Zuchairah, M.T. Pailthorpe, S.K. David, *Text. Res. J.* 67 (1997) 69.
- [36] D. Biniaś, A. Włochowicz, W. Biniaś, *Fibers Text. East. Eur.* 12 (2004) 46.
- [37] S. Wu, *Polymer Interface and Adhesion*, Marcel Dekker, Inc, New York, 1982.
- [38] N.S. Murthy, M. Stamm, J.P. Sabilia, S. Krimms, *Macromolecules* 22 (1989) 1261.